



## EFFECT OF SR CONTENT ON THE MICROSTRUCTURE DEVELOPMENT AND ELECTROCHEMICAL PERFORMANCE OF $La_{1-x}Sr_xMnO_3$ FILMS

Mahla SHAHSAVAR GOCMEN<sup>1</sup>, Ayca EKSIOGLU<sup>2\*</sup>, Aligul BUYUKAKSOY<sup>3</sup>

<sup>1</sup> Yeditepe University, Engineering Faculty, Materials Science and Nanotechnology Engineering, Istanbul, Türkiye

<sup>2,3</sup> Gebze Technical University, Engineering Faculty, Materials Science and Engineering, Kocaeli, Türkiye

### Keywords

*Thin Films,  
Polymeric Precursors,  
Perovskite Cathode,  
Strontium Segregation,  
Electrochemical Performance.*

### Abstract

Strontium doped lanthanum manganite ( $La_{1-x}Sr_xMnO_3$  -LSM) is the conventionally used oxygen reduction electrocatalyst in solid oxide fuel cell cathodes. In recent years, Sr-segregation at the LSM surface has been shown to occur and limit oxygen reduction performance. Therefore, the effect of Sr-doping on the microstructure development and performance of liquid precursor-derived LSM film electrodes with different Sr-contents was investigated in this study. It was found that as Sr content increased, LSM structure became amorphous, which is beneficial for the electrochemical performance. Despite this fact, the undoped  $LaMnO_3$  film performed better in comparison to heavily Sr-doped LSM, likely because of Sr-segregation at the Sr-doped electrode surface. These results suggested that trying to avoid Sr doping in  $LaMnO_3$  electrodes may be a good strategy if its microstructural instability could be addressed, to achieve high performance solid oxide fuel cell cathodes.

## STRONSIYUM KATKISININ $La_{1-x}Sr_xMnO_3$ FİMLERİNİN MİKROYAPI GELİŞİMİ VE ELEKTROKİMYASAL PERFORMANSI ÜZERİNE ETKİSİ

### Anahtar Kelimeler

*İnce Filmler,  
Polimerik Öncüller,  
Perovskit Katot,  
Stronsiyum Segregasyonu,  
Elektrokimyasal Performans.*

### Öz

Stronsiyum katkılı lantanyum manganiz oksit ( $La_{1-x}Sr_xMnO_3$  -LSM), katı oksit yakıt hücresi katotlarında geleneksel olarak kullanılan oksijen indirgenme elektrokatalizörüdür. Son yıllarda LSM yüzeylerinde Sr birikmesi meydana geldiği ve bunun oksijen indirgenme reaksiyonunu engellediği gözlemlenmiştir. Bu sebeple, bu çalışmada sıvı çözelti temelli yöntemlerle üretilen LSM film elektrotlarında Sr-katkısının mikroyapı gelişimi ve performans üzerine etkisi çalışılmıştır. Sr katkı miktarı arttıkça LSM yapısının performansı arttıracak şekilde amorflaştığı görülmüştür. Fakat buna rağmen, katkısız  $LaMnO_3$  filminin, yüksek miktarda Sr katkısı içeren LSM filmine göre daha yüksek performans gösterdiği tespit edilmiştir. Bunun da yüksek miktarda Sr içeren LSM filminin yüzeyinde Sr segregasyonu meydana gelmesinden kaynaklandığı hipotezi oluşturulmuştur. Bu sonuçlar, yüksek performans gösteren katı oksit yakıt hücresi katotlarının elde edilebilmesi için  $LaMnO_3$  elektrotlarında mikroyapı kararlılığı sağlanabildiği takdirde Sr-katkısından kaçınılmasının verimli bir strateji olabileceğini göstermektedir.

### Alıntı / Cite

Shahsavat Gocmen, M., Eksioğlu, A., Buyukaksoy, A., (2024). Effect of Sr Content on the Microstructure Development and Electrochemical Performance of  $La_{1-x}Sr_xMnO_3$  Films, Journal of Engineering Sciences and Design, 12(4), 653-662.

### Yazar Kimliği / Author ID (ORCID Number)

M. Shahsavat Gocmen, 0000-0002-7223-2607  
A. Eksioğlu, 0000-0003-2941-0591  
A. Buyukaksoy, 0000-0003-2227-8938

### Makale Süreci / Article Process

|                                  |            |
|----------------------------------|------------|
| Başvuru Tarihi / Submission Date | 23.10.2023 |
| Revizyon Tarihi / Revision Date  | 09.09.2024 |
| Kabul Tarihi / Accepted Date     | 14.10.2024 |
| Yayın Tarihi / Published Date    | 25.12.2024 |

\* İlgili yazar / Corresponding author: aycaeksioglu@gmail.com, +90-262-605-2662

## EFFECT OF SR CONTENT ON THE MICROSTRUCTURE DEVELOPMENT AND ELECTROCHEMICAL PERFORMANCE OF $La_{1-x}Sr_xMnO_3$ FILMS

Mahla SHAHSAVAR GOCMEN<sup>1</sup>, Aycan EKSIÖGLÜ<sup>2†</sup>, Aligul BUYUKAKSOY<sup>3</sup>,

<sup>1</sup> Yeditepe University, Engineering Faculty, Materials Science and Nanotechnology Engineering, Istanbul, Türkiye

<sup>2,3</sup> Gebze Technical University, Engineering Faculty, Materials Science and Engineering, Kocaeli, Türkiye

---

### Highlights

- The necessity of Sr-doping in LSM electrocatalysts was investigated.
- Strontium segregates at the outer surface of LSM, causing the formation of insulating SrO phase.
- As Sr content increases, crystallinity decreases and electrochemical performance decreases.

---

### Purpose and Scope

The aim of the paper is to investigate the correlation between the Sr content in LSM and the Electrochemical Performance and to reevaluation the necessity of Sr doping to LSM electrocatalyst.

### Design/methodology/approach

To investigate the necessity of Sr content in LSM, three types of  $La_{1-x}Sr_xMnO_3$  ( $x=0$ ,  $x=0.2$  and  $x=0.4$ ) films were prepared using polymeric precursors. Microstructure and electrochemical performance of cathodes were investigated by scanning electron microscopy and electrochemical impedance spectroscopy, respectively.

### Findings

As Sr content increased, crystallinity decreased, which decreased electrochemical performance. This result suggested that Sr doping may not be required for high performance if nanocomposite electrodes with Sr-free LSM could be fabricated.

### Originality

We investigate the effect of Sr content in LSM thin film cathodes fabricated by polymeric precursor method on the microstructure evolution and electrochemical performance for the first time in the literature.

---

<sup>†</sup> Corresponding author: aycaneksioglu@gmail.com, +90-262-605-2662

## 1. Introduction

Solid oxide fuel cells (SOFCs) are devices that convert to chemical energy to electrical energy with high efficiency (up to %80). A typical SOFC consists of three main components known as anode, cathode, and electrolyte. Oxygen reduction and hydrogen oxidation reactions take place at the cathode and anode, respectively (Cooper and Brandon, 2017). Anode and cathode materials need to have high electrical conductivity, high catalytic activity for electrochemical reactions and must be compatible with other cell components (Cooper *et al.*, 2017).

Strontium doped lanthanum manganite ( $\text{La}_x\text{Sr}_{1-x}\text{MnO}_3$ , LSM) is the conventional and most widely investigated cathode material for SOFCs. Partial substitution of lanthanum with strontium is considered to lead to hole formation, which, in turn, results in high electronic conductivity [Ping Jiang, 2008; Branković *et al.*, 2010]. LSM is mainly used in the form of a composite with the generic ionic conductor material – yttria stabilized zirconia (YSZ), which leads to the formation of electrocatalyst – ionic conductor – gas (pore) triple phase boundaries where the electrochemical reactions predominantly take place (Kenji and Nishiya, 1992; Perry Murray and Barnett, 2001; Tsai and Barnett, 1997; Østergård *et al.*, 1995; Song *et al.*, 2007).

A significant problem with LSM and similar perovskite materials with  $\text{Sr}^{2+}$  substitutions at  $\text{La}^{3+}$  sites is that due to the larger ionic radius of  $\text{Sr}^{2+}$  in comparison to that of  $\text{La}^{3+}$  and the electrostatic attraction of oxygen vacancies at the surface,  $\text{Sr}^{2+}$  segregates to the outer surface and forms resistive  $\text{SrO}/\text{Sr}(\text{OH})_2/\text{SrCO}_3$  species, causing performance degradation when subjected to high temperatures during fabrication or operation (Eksioglu *et al.*, 2019; Cai *et al.*, 2012; van der Heide *et al.*, 2002; Majkic *et al.*, 2004; Yu *et al.*, 2016; Khan *et al.*, 2021; François *et al.*, 2021; Niu *et al.*, 2021; Hong *et al.*, 2021). This phenomenon has been observed in many forms of similar materials, namely, pulsed laser deposition (PLD) derived  $\text{La}_{0.8}\text{Sr}_{0.2}\text{CoO}_{3-\delta}$  (LSC) and LSM films (Kubicek *et al.*, 2011; Lee *et al.*, 2013; Huber *et al.*, 2012), bulk (La, Sr) (Co, Fe) $\text{O}_3$  (LSCF) ceramics (Oh *et al.*, 2012) and porous LSM electrodes fabricated by screen printing/sintering (Caillol *et al.*, 2007). More recently, our attempts on the fabrication of LSM-samarium doped ceria (LSM-SDC) nanocomposite electrodes from a single polymeric precursor has also revealed the formation of a thin SrO top layer (Eksioglu *et al.*, 2019). Switching the divalent Sr dopant to Ca reduced the dopant segregation amount and consequently, increased the performance but did not eliminate dopant segregation entirely (Eksioglu *et al.*, 2019).

In the present work, we investigate the effect of Sr content in LSM thin films fabricated by polymeric precursor method on the microstructure evolution and electrochemical performance for the first time in the literature. X-ray diffraction method was used for phase determination and scanning electron microscopy and electrochemical impedance spectroscopy were used for investigation of microstructure and electrochemical performance of cathodes, respectively. Previously, Turkey *vd.*, investigated the effects of Sr content on the optical, electrical and magnetic properties of LSM, but they have not investigated their high temperature oxygen reduction properties (Turkey *et al.*, 2017). The results of this study show us that the necessity of Sr-doping into  $\text{LaMnO}_3$  perovskite materials may need to be re-considered for solid oxide fuel cell cathode applications.

## 2. Experimental Section

### 2.1. Fabrication of LSM Films

Polymeric precursor method was used to prepare thin film electrodes. Polymeric  $\text{La}_{1-x}\text{Sr}_x\text{MnO}_3$  ( $x=0, 0.2$  and  $0.4$ ) precursors were prepared by dissolving metal salts,  $\text{La}(\text{NO}_3)_3 \cdot 6\text{H}_2\text{O}$  ( $\geq 99$ , Fluka),  $\text{Mn}(\text{NO}_3)_2 \cdot 4\text{H}_2\text{O}$  ( $\geq 99$ , Sigma-Aldrich), and  $\text{Sr}(\text{NO}_3)_2 \cdot \text{H}_2\text{O}$  ( $\geq 99$ , Sigma-Aldrich) in 10 gr distilled water and 10 gr ethylene glycol ( $\text{C}_2\text{H}_6\text{O}_2$ ) added into the aqueous solution. Cation to ethylene glycol molar ratio was kept at 0.02. Then, to remove all the water and allow for polymerization, the solution was kept on the magnetic stirrer at  $80^\circ\text{C}$  and the total weight of the solution was frequently measured with time. When the total weight loss was equal to the water amount in the solution (added water + crystalline water present in the nitrates) the process was ended. To improve the wetting quality of the precursors, 10 gr of 2-butoxyethanol was added to the solution. The synthesized polymeric precursors were applied onto the yttria stabilized zirconia (YSZ) electrolyte substrate via spin coating. The YSZ substrates were produced by die pressing of YSZ powders (Tosoh Corp., 8 mol % yttria) and their subsequent sintering for four hours at a temperature of  $1400^\circ\text{C}$ . LSM precursor depositions onto the YSZ substrates were carried out at 3000 rpm spinning speed. The coated film was dried by heating on a hot plate from  $50$  to  $350^\circ\text{C}$  slowly to avoid crack formations. This deposition/drying cycle was performed fifteen times to get the appropriate cathode layer thickness. As a result, a solid, well-adhering, amorphous film was obtained on the YSZ substrate. LSM depositions have been applied to both sides of the electrolyte substrate to achieve symmetrical half-cells in the electrode/electrolyte/electrode arrangement. The three types of samples with  $\text{La}_{1-x}\text{Sr}_x\text{MnO}_3$  ( $x=0, 0.2$  and  $0.4$ ) compositions were coded as LSM-0, LSM-02 and LSM-04, respectively. The complete fabrication route is visually illustrated in Figure 1.

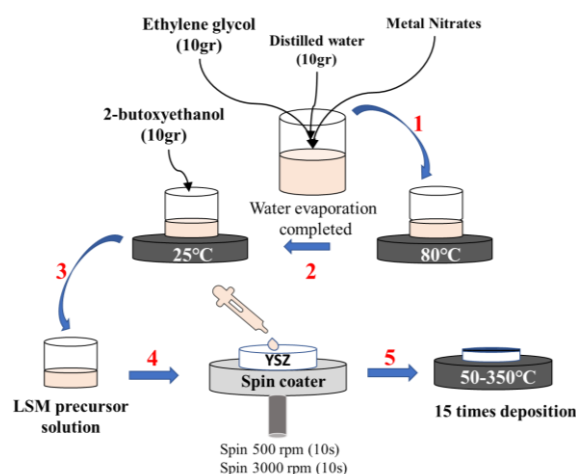


**Figure 1.** Schematic diagram of LSM thin film cathode fabrication using polymeric precursor method

## 2.2. Thermal Characterization

Differential thermal analyses and thermal gravimetric analyses (Netzsch STA 449 F3 at 30-800 °C) were used for the thermal analyses of LSM gels.

## 2.3. Structural Characterization

Phase analyses of fabricated LSM films on YSZ electrolyte substrates were investigated using X-ray diffraction (XRD, Rigaku D/max 2200) method using Cu K $\alpha$  radiation. XRD measurements were performed on LSM thin film cathodes after heat treatment at 500, 600 and 700 °C for 2 hours and after 100-hour exposure to 700 °C.

## 2.4. Microstructural Characterization

Evolution of film microstructure was determined by scanning electron microscopy (SEM) after annealing the specimens at specified temperatures (500, 600 and 700 °C) for the period of two hours. Further SEM analyses were carried out after 100 hours of exposure to 700 °C. SEM analyses were performed using Philips XL 30 S FEG.

## 2.5. Electrochemical Characterization

The electrochemical characterization of electrode films was carried out to investigate the oxygen reduction rate on LSM electrode films by electrochemical impedance spectroscopy (EIS), which allows the detection of resistive and capacitive elements of electrochemical processes with different time constants. To perform EIS measurements, symmetrical half-cell samples were prepared by applying the silver paste onto both electrode surfaces using a brush and drying on a hot plate at 120 °C. Silver did not block the LSM surface because the deposited Ag layer is porous, which allows oxygen gas transportation to the LSM surface (Demirkal and Buyukaksoy, 2019). Later, for generating the electrical connection, silver wires were attached to the silver current collectors with ceramic adhesive paste. The electrical contacts were placed onto the films and the EIS measurements were commenced. The EIS analyses were performed at 700 °C, in air, which, considering that LSM films were not exposed to temperatures higher than 350 °C, meant that the films underwent heat treatment in situ.

## 3. Results and Discussion

### 3.1. Thermal Analysis

Effect of Sr content on the thermal behaviour of the LSM ( $\text{La}_{1-x}\text{Sr}_x\text{MnO}_3$ ;  $x=0, 0.2$  or  $0.4$ ) precursors was investigated via DTA-TGA analyses performed on gels dried from polymeric solutions (Figure 2). A significant mass loss accompanied by an exothermic peak was observed at two temperatures, one at around 200 °C and the other at around 450 °C in all samples (Figures 2a-c). Evidently, with increasing Sr content, the amount of mass loss at 200 °C decreased, while that at 450 °C increased (Figures 2a-c). Eksioğlu *et al* investigated the effects of nitric acid addition on the properties of similar polymeric precursors and reported that the sharp mass loss at 200 °C was caused by the burnout of organics, which evolved into a more gradual mass loss at a temperature range of 200-400 °C upon enhanced degree of polymerization (Eksioğlu *et al.*, 2023). In the present case, it is possible that Sr

addition somehow enhanced the degree of polymerization and allowed for a more gradual mass loss, rather than an abrupt one at 200 °C. 700-800 °C region in the DTA-TGA plots also exhibit dependency on the Sr content. While LSM-02 and more pronouncedly LSM-04 exhibit weight losses in this region, LSM-0 does not undergo such a process within this temperature range. In the literature, Stevenson *et al.*, also reported that perovskites exhibited a weight loss at the 600-1000 °C, which shifted to lower temperatures and became more pronounced with increasing Sr content (Stevenson *et al.*, 1996). This was linked to oxygen loss, *i.e.*, increasing  $\delta$  in  $(La, Sr) MnO_{3-\delta}$ , which corresponds to formation of oxygen vacancies (Stevenson *et al.*, 1996).

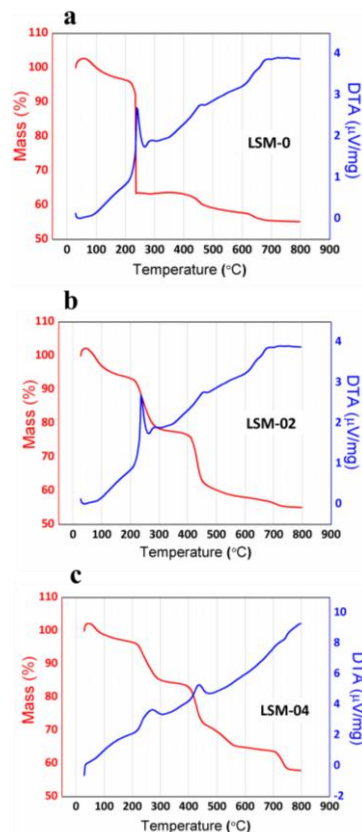


**Figure 2.** DTA-TGA curves of LSM gels

### 3.2. Phase Analysis

X-ray diffraction (XRD) analyses were carried out on LSM films on YSZ substrates after heat treatment at 500, 600 and 700 °C for 2 hours and upon a 100-hour exposure to 700 °C. For facile comparison of the crystallinities of different samples, XRD data were plotted so as to make sure that the maximum value of the vertical axis is 20% higher than the peak value of the highest intensity peak. Only YSZ peaks coming from electrolyte substrate were observed in XRD patterns of LSM-0 samples after heat treatment at 500 or 600 °C (Figure 3a). Increasing the heat treatment temperature to 700 °C resulted in the formation of rhombohedral phase (Figure 3a). The intensity of the most intense peak of this phase was similar to that of the YSZ electrolyte (Figure 3a). In the case of LSM-02, crystallization of the rhombohedral phase was also possible only at 700 °C, but in this case, the intensity of the most intense peak of the rhombohedral phase was *ca.* half that of the electrolyte (Figure 3b), indicating a smaller degree of crystallization in comparison to that of LSM-0 (assuming similar thickness and porosity). In the case of LSM-04, no peaks belonging to LSM was found, suggesting that the LSM phase remained amorphous (Figure 3c). These results suggest that Sr doping inhibits the crystallization of LSM from liquid precursors in this condition. It should also be noted that the resistive phases that form at the LSM electrode/YSZ electrolyte interfaces (such as  $La_2Zr_2O_7$ ) when conventional high-temperature fabrication techniques are used (Mitterdorfer and Gauckler, 1998) were not detected in the present case, likely due to the lower fabrication temperature used in the present case (*i.e.*, 700 °C).

Upon long-term annealing, LSM-04 remained amorphous, while the YSZ / LSM peak intensity ratio increased in the case of LSM-0. The ratio of the YSZ and LSM peaks indicates how much signal is detected from the LSM film and the YSZ substrate. This phenomenon likely originated from the pore formation at the grain boundaries of LSM-0 and the solid-state de-wetting of the LSM film, which exposed the YSZ substrate surface and hence, allowed a higher intensity of x-rays diffracted from the YSZ substrate to arrive at the detector. In the literature, Turkey *et al.*

investigated the effect of Sr content on the phase formation of  $\text{La}_{1-x}\text{Sr}_x\text{MnO}_3$  powders synthesized by citrate gel method (Turky *et al.*, 2017). They have found that the perovskite phase formed even when  $x=0.2$ . The discrepancy between their study and the present one likely originated from the high calcination temperatures (800-1000 °C) they utilized (Turky *et al.*, 2017).

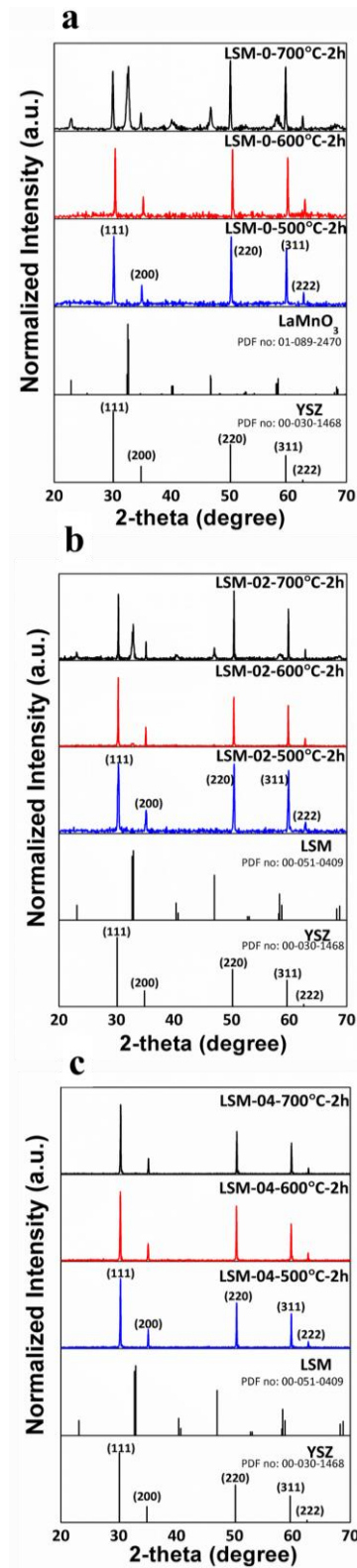


**Figure 3.** XRD patterns of a) LSM-0, b) LSM-02 and c) LSM-04 thin film cathodes after heat treatment at 500 °C, 600 °C and 700 °C for 2 hours

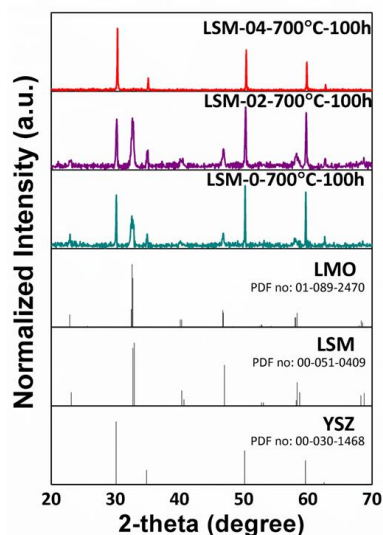


**Figure 4.** XRD patterns of LSM-0, LSM-02 and LSM-04 thin film cathodes after heat treatment at 700 °C for 100 hours

### 3.3. Microstructural Analysis

Figure 5 shows SEM images of the top surfaces of YSZ substrate (Figure 5a) and LSM films after heat treatment at 500, 600 and 700 °C for 2 hours and after 100 hours of heat treatment at 700 °C, in air (Figure 5b-m). Particles with diameters of ca. 125 nm were observed on the surface of LSM-0 film, which, otherwise had a featureless morphology after heat treatment at 500 °C for 2 hours (Figure 5b). With increasing heat treatment temperature, the surface particles disappeared, and nucleation and growth of grains took place (Figure 5c and d). A similar trend was observed in the case of LSM-02, but with a more limited grain growth achieved at 700 °C (Figures 5f-h). No grain formation was identified in the case of LSM-04 films, regardless the heat treatment temperature (Figures 5j-l). 100-hour exposure to 700 °C did not cause significant microstructural change in LSM-02 and LSM-04. On the other hand, significant grain growth and even separation of grains at grain boundaries due to solid-state dewetting was observed in the case of LSM-0 (Figures 5e, i, m). In general, the formation and growth trends of grain were in agreement with the XRD results.

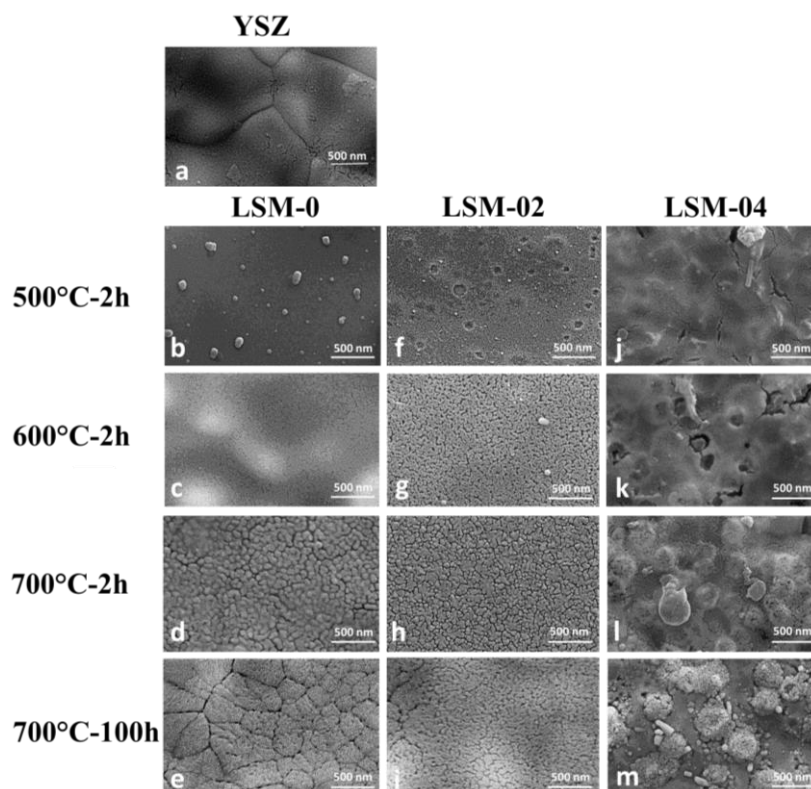


**Figure 5.** Top surface SEM images of a) YSZ and b-m) LSM films heat treated at 500 – 700 °C, in air for either 2 or 100 hours

### 3.4. Electrochemical Analysis

To investigate the electrochemical performances of thin film cathodes, EIS analyses were performed on symmetrical half-cells in the electrode/electrolyte/electrode configuration at 700 °C. Figure 6 shows the Nyquist and Bode (inset) plots of thin film electrodes. Ohmic resistances were excluded from the data for easy comparison. Thus, the distance from the origin to the horizontal intercept gives the area specific polarization resistance (ASR) of the two electrodes. Hence, to determine the area specific polarization resistance per cathode ( $ASR_{cathode}$ ), ASR must be divided by two.

LSM-0 and LSM-02 yielded similar  $ASR_{cathode}$  values of ca. 1.5  $\Omega \cdot \text{cm}^2$  at 700 °C, while LSM-04 exhibited a lower electrochemical performance of ca. 3.5  $\Omega \cdot \text{cm}^2$  at the same temperature (Figure 6). Figure 7 shows the change in  $ASR_{cathode}$  upon prolonged exposure to 700 °C.

The widely accepted notion is that substituting La with Sr generates a negative effective charge ( $La'_{Sr}$ ), which induces the oxidation of  $Mn^{3+}$  into  $Mn^{4+}$ , generating electron holes ( $Mn_{Mn}$ ), which, results in p-type conductivity and high electrochemical performance (Jiang, 2019). Therefore, higher Sr content should correspond to higher electrochemical activity. In addition, literature reports suggest that amorphous structure in Sr-doped perovskites (as in the case of LSM-04) is more beneficial in comparison to the crystalline structure, because it has a more open structure, which facilitates oxygen ion diffusion and the weaker transition metal – oxygen bonds induce oxygen vacancy formation, thereby facilitating oxygen adsorption and migration (Cavallaro *et al.*, 2018). Therefore, in the present case, considering the above-mentioned advantages of its amorphous structure, LSM-04 is expected to exhibit the highest electrochemical performance. However, Figure 6 shows that LSM-0 is the electrode that exhibited the highest initial electrochemical performance, which is counterintuitive. Our hypothesis is that this phenomenon can be explained by the Sr segregation that occurs rapidly during the fabrication process in LSM-02 and LSM-04 samples, forming surface  $SrO/Sr(OH)_2/SrCO_3$  species that block oxygen adsorption to the surface (Koo *et al.*, 2018).

In the performance stability tests, LSM-0 and LSM-02 exhibited similar performance degradation rates, while the electrochemical performance of LSM-04 was more stable in comparison to the other samples (Figure 7). Since LSM-0 did not contain Sr, its performance degradation could not be due to Sr segregation. Meanwhile, the microstructural analyses in Figure 5 showed a significant grain growth and even de-wetting at grain boundaries in LSM-0 upon prolonged heat treatment, which should induce performance loss. LSM-04 had not crystallized throughout the 100-hour exposure to 700 °C, hence, grain growth and grain separation at grain boundaries did not take place, constituting an unchanged microstructure (Figure 5). It is likely that Sr segregation at the top surface continued to take place, blocking surface adsorption of oxygen and causing performance loss. Although not to the extent of LSM-0, LSM-02 has also shown grain growth (Figure 5). As it also contains Sr, some surface segregation (likely to a lesser extent in comparison to the case of LSM-04) is expected. Therefore, a combined effect of microstructural and surface-chemical degradation caused the performance loss in LSM-02.

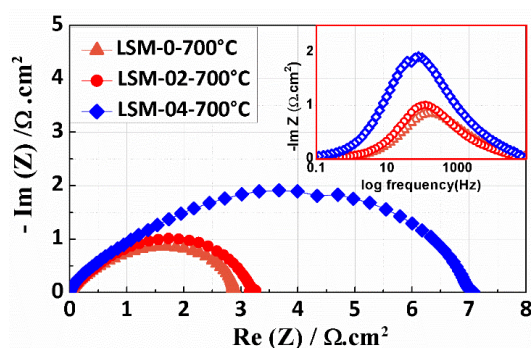


**Figure 6.** Nyquist plot showing the electrochemical impedance spectra of LSM-0, LSM-02 and LSM-04 thin film cathodes on YSZ substrates

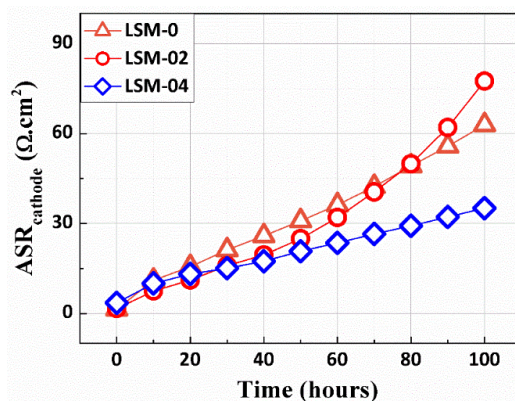


**Figure 7.** Area specific resistances as a function of time of LSM-0, LSM-02 and LSM-04 thin films at 700 °C

#### 4. Summary

In this study, we aimed to investigate the effect of strontium content on the microstructural evolution and electrochemical performance of the widely used SOFC cathode material – LSM – in thin film form. We fabricated LSM cathodes using polymeric precursors with different amount of strontium and investigated the phase and microstructure evolution of the fabricated electrodes and correlated these to electrochemical performance. XRD and SEM analyses respectively revealed that increasing Sr content increased the crystallization temperature and inhibited grain growth. EIS analyses showed that initially, increasing Sr content in LSM resulted in lower electrochemical performance, while the perovskite which contained no Sr exhibited the highest electrochemical performance. It was hypothesized that this counter-intuitive phenomenon originated from a possible Sr-segregation at the surfaces of Sr-containing samples. Long-term performance tests conducted at 700 °C revealed that the sample with the highest Sr amount had the most stable performance, likely due to its relatively stable microstructure, i.e., it remained amorphous throughout all heat treatment procedures. Undoped perovskite film electrode underwent significant grain growth and showed signs of solid-state de-wetting, and consequently exhibited extensive performance loss upon long-term exposure to 700 °C.

Based on the results of this study, it can be suggested that increasing Sr-content does not correspond to higher electrochemical performance in LaMnO<sub>3</sub> electrodes, at least for those fabricated in the film form through polymeric precursor-based methods. Deeper surface-chemical analyses of LaMnO<sub>3</sub> electrode films with varying Sr-contents and pre-heat treatment conditions are now underway to test our hypothesis that Sr surface segregation is the origin of the initial poor performance of highly Sr-doped LaMnO<sub>3</sub> film electrodes.

#### Conflict of Interest

No conflict of interest was declared by the authors.

#### References

- Branković, Z., Đuriš, K., Radojković, A., Bernik, S., Jagličić, Z., Jagodič, M., Vojisavljević, K., Branković, G., 2010. Magnetic properties of doped LaMnO<sub>3</sub> ceramics obtained by a polymerizable complex method. *Journal of Sol-Gel Science and Technology*, vol. 55, pp. 311-316.
- Cai, Z., Kubicek, M., Fleig, J., Yildiz, B., 2012. Chemical heterogeneities on La<sub>0.6</sub>Sr<sub>0.4</sub>CoO<sub>3-δ</sub> thin films-correlations to cathode surface activity and stability. *Chemistry of Materials*, vol. 24, no. 6, pp. 1116-1127.
- Caillol, N., Pijolat, M., Siebert, E., 2007. Investigation of chemisorbed oxygen, surface segregation and effect of post-treatments on La<sub>0.8</sub>Sr<sub>0.2</sub>MnO<sub>3</sub> powder and screen-printed layers for solid oxide fuel cell cathodes. *Applied Surface Science*, vol. 253, no. 10, pp. 4641-4648.
- Cavallaro, A., Pramana, S. S., Ruiz-Trejo, E., Sherrell, P. C., Ware, E., Kilner, J. A., Skinner, S. J., 2018. Amorphous-Cathode-Route towards Low Temperature. *Sustainable Energy Fuels*, vol. 2, pp. 862-875
- Cooper, S.J., Brandon, N. P., 2017. Chapter 1 - An Introduction to Solid Oxide Fuel Cell Materials, Technology and Applications, Editor(s): Nigel P. Brandon, Enrique Ruiz-Trejo, Paul Boldrin, *Solid Oxide Fuel Cell Lifetime and Reliability*, Academic Press.
- Demirkal, E., Buyukaksoy, A., 2019. Effect of frit content in the silver current collector inks on the electrochemical performance of solid oxide fuel cell cathodes. *Journal of Engineering Sciences and Design*, vol. 7, no. 4, pp. 796-802.
- Eksioglu, A., Arslan, L. C., Sezen, M., Ow-Yang, C., Buyukaksoy, A., 2019. Formation of nanocomposite solid oxide fuel cell cathodes by preferential clustering of cations from a single polymeric precursor. *ACS Applied Materials & Interfaces*, vol. 11, no. 51, pp. 47904-47916.
- Eksioglu, A., Sakir, I. A., Buyukaksoy, A., 2022. Formation mechanism of large porosity in solid oxide cell electrode coatings fabricated using ethylene glycol-based precursor solutions and its impact on the electrochemical performance. *Ceramics International*, vol. 49, no. 1, pp. 956-963.

- François, M., Carpanese, M. P., Heintz, O., Lescure, V., Clematis, D., Combemale, L., Demoisson, F., Caboche, G., 2021. Chemical degradation of the  $\text{La}_{0.6}\text{Sr}_{0.4}\text{Co}_{0.2}\text{Fe}_{0.8}\text{O}_{3-\delta}$  interface during sintering and cell operation. *Energies*, vol. 14, no. 12, pp. 3674.
- Hong, J., Anisur, M. R., Heo, S. J., Dubey, P. K., Singh, P., 2021. Sulphur poisoning and performance recovery of SOFC air electrodes. *Frontiers in Energy*, vol. 9, pp. 643431.
- Huber, A-K., Falk, M., Rohnke, M., Luerssen, B., Amati, M., Gregoratti, L., Hesse, D., Janek, J., 2012. In situ study of activation of LSM fuel cell cathodes-electrochemistry and surface analysis of thin-film electrodes. *Journal of Catalysis*, vol. 294, pp. 79-88.
- Jiang, S. P., 2019. Development of lanthanum strontium cobalt ferrite perovskite electrodes of solid oxide fuel cells-A review. *International Journal of Hydrogen Energy*, vol. 44, no. 14, pp. 7448-7493.
- Kenji, T., Nishiya, M., 1992.  $\text{LaMnO}_3$  air cathodes containing  $\text{ZrO}_2$  electrolyte for high temperature solid oxide fuel cells. *Solid State Ionics*, vol. 57 no. 3-4, 295-302.
- Khan, M. Z., Iltaf, A., Ishfaq, H. A., Khan, F. N., Tanveer, W. H., Song, R-H., Mehraan, M. T., Saleem, M., Hussain, A., Masaud, Z., 2021. Flat-tubular solid oxide fuel cells and stacks: a review. *Journal of Asian Ceramic Societies*, vol. 9, no. 3, pp. 745-770.
- Koo, B., Kim, K., Kim, J. K., Kwon, H., Han, J. W., Jung, W., 2018. Sr Segregation in Perovskite Oxides: Why It Happens and How It Exists. *Joule*, vol. 2, pp. 1476-1499.
- Kubicek, M., Limbeck, A., Frömling, T., Hutter, H., Fleig, J., 2011. Relationship between cation segregation and the electrochemical oxygen reduction kinetics of  $\text{La}_{0.6}\text{Sr}_{0.4}\text{CoO}_{3-\delta}$  thin film electrodes. *Journal of the Electrochemical Society*, vol. 158 no. 6, pp. B727.
- Lee, W., Han, J. W., Chen, Y., Cai, Z., Yildiz, B., 2013. Cation size mismatch and charge interactions drive dopant segregation at the surfaces of manganite perovskites. *Journal of the American Chemical Society*, vol. 135, no. 21, pp. 7909-7925.
- Majkic, G., Mironova, M., Wheeler, L. T., Salama, K., 2004. Stress-induced diffusion and defect chemistry of  $\text{La}_{0.2}\text{Sr}_{0.8}\text{Fe}_{0.8}\text{Cr}_{0.2}\text{O}_{3-\delta}$ : structural, elemental and chemical analysis. *Solid State Ionics*, vol. 167, no. 3-4, pp. 243-254.
- Mitterdorfer, A., Gauckler, L. J., 1998.  $\text{La}_2\text{Zr}_2\text{O}_7$  formation and oxygen reduction kinetics of the  $\text{La}_{0.85}\text{Sr}_{0.15}\text{Mn}_y\text{O}_2(\text{g})|\text{YSZ}$  system. *Solid State Ionics*, vol. 111, no. 3-4, pp. 185-218.
- Niu, Y., Zhou, Y., Lv, W., Chen, Y., Zhang, Y., Zhang, W., Luo, Z., Kane, N., Ding, Y., Soule, L., Liu, Y., He, W., Liu, M., 2021. Enhancing oxygen reduction activity and Cr tolerance of solid oxide fuel cell cathodes by a multiphase catalyst coating. *Advanced Functional Materials*, vol. 31, no. 19, pp. 2100034.
- Oh, D., Gostovic, D., Wachsman, E. D., 2012. Mechanism of  $\text{La}_{0.6}\text{Sr}_{0.4}\text{Co}_{0.2}\text{Fe}_{0.8}\text{O}_3$  cathode degradation. *Journal of Materials Research*, vol. 27, pp. 1992-1999.
- Perry Murray, E., Barnett, S. A., 2001.  $(\text{La, Sr})\text{MnO}_3\text{-(Ce,Gd)}\text{O}_{2-x}$  composite cathodes for solid oxide fuel cells. *Solid State Ionics*, vol. 143 no. 3-4, pp. 265-273.
- Ping Jiang, S., 2008. Development of lanthanum strontium manganite perovskite cathode materials of solid oxide fuel cells: a review. *Journal of Materials Science*, vol. 43, pp. 6799-6833.
- Song, H. S., Kim, W. H., Hyun, S. H., Moon, J., Kim, J., Lee, H-W., 2007. Effect of starting particulate materials on microstructure and cathodic performance of nanoporous LSM-YSZ composite cathodes. *Journal of Power Sources*, vol. 167, no. 2, pp. 258-264.
- Stevenson, J. W., Armstrong, T. R., Carneim, R. D., Pederson, L. R., Weber, W. J., 1996. Electrochemical Properties of Mixed Conducting Perovskites  $\text{La}_{1-x}\text{M}_x\text{Co}_{1-y}\text{Fe}_y\text{O}_{3-\delta}$  (M= Sr, Ba, Ca). *Journal of the Electrochemical Society*, vol. 143, pp. 2722.
- Tsai, T., Barnett, S. A., 1997. Effect of LSM-YSZ cathode on thin-electrolyte solid oxide fuel cell performance. *Solid State Ionics*, vol. 93, no. 3-4, pp. 207-217.
- Turky, A. O., Rashad, M. M., Hassan, A. M., Elnaggar, E. M., Bechelany M., 2017. Optical, electrical and magnetic properties of lanthanum strontium manganite  $\text{La}_{1-x}\text{Sr}_x\text{MnO}_3$  Synthesized Through the Citrate Combustion Method. *Physical Chemistry Chemical Physics*, vol. 19, 6878-6886.
- Van der Heide, P. A. W., 2002. Systematic x-ray photoelectron spectroscopy study of  $\text{La}_{1-x}\text{Sr}_x$ -based perovskite-type oxides. *Surface and Interface Analysis*, vol. 33, no. 5, pp. 414-425.
- Yu, Y., Ludwig, K. F., Woicik, J. C., Gopalan, S., Pal, U. B., Kaspar, T. C., Basu, S. N., 2016. Effect of Sr content and strain on Sr surface segregation of  $\text{La}_{1-x}\text{Sr}_x\text{Co}_{0.2}\text{Fe}_{0.8}\text{O}_{3-\delta}$  as cathode material for solid oxide fuel cells. *ACS Applied Materials & Interfaces*, vol. 8, no. 40, pp. 26704-26711
- Østergård, M. J. L., Clausen, C., Bagger, C., Mogensen, M., 1995. Manganite-zirconia composite cathodes for SOFC: Influence of structure and composition. *Electrochimica Acta*, vol. 40, no. 12, pp. 1971-198.